

Nanoscale Probing of Adsorbed Species by Tip-Enhanced Raman Spectroscopy

Bruno Pettinger,^{1,*} Bin Ren,^{1,2} Gennaro Picardi,¹ Rolf Schuster,¹ and Gerhard Ertl¹

¹*Fritz-Haber-Institut der Max-Planck-Gesellschaft, Faradayweg 4-6, D-14195 Berlin, Germany*

²*Department of Chemistry, Xiamen University, Xiamen 361005, China*

(Received 14 November 2003; published 2 March 2004)

Tip-enhanced Raman spectroscopy (TERS) is based on the optical excitation of localized surface plasmons in the tip-substrate cavity, which provides a large but local field enhancement near the tip apex. We report on TERS with smooth single crystalline surfaces as substrates. The adsorbates were CN^- ions at Au(111) and malachite green isothiocyanate (MGITC) molecules at Au(111) and Pt(110) using either Au or Ir tips. The data analysis yields Raman enhancements of about 4×10^5 for CN^- and up to 10^6 for MGITC at Au(111) with a Au tip, probing an area of less than 100 nm radius.

DOI: 10.1103/PhysRevLett.92.096101

PACS numbers: 68.37.Uv, 33.20.Fb, 68.43.Pq, 73.20.Mf

Scanning probe techniques are powerful tools for studying the morphology of surfaces down to the atomic scale. However, their use also for spectroscopic identification of surface species has thus far been limited to a few special cases, STM-inelastic electron tunneling spectroscopy (STM-IETS) being the most prominent example [1,2]. One important property of STM-IETS is the high spatial resolution, which thus permits studies with single molecules. Some near-field optical spectroscopies exhibit similar sensitivity [3–6]. However, these techniques are based on the use of fluorescent labels and thus provide only indirect information about the species probed.

In this respect, promising aspects are offered by tip-enhanced Raman spectroscopy (TERS) as an apertureless optical near-field technique [7–14]. The tip of an atomic force microscopy (AFM) or a scanning tunneling microscopy (STM) device provides a locally confined appreciable enhancement of the electromagnetic field of an incoming light wave, thus causing the enhanced Raman scattering from a narrow section of the surface area. In addition, TERS overcomes, in principle, the two obstacles of the standard surface-enhanced Raman spectroscopy (SERS), namely, the need for nonplanar (rough) surfaces and its restriction to specific adsorbates. Additionally, the Raman enhancement can be probed at any location of the sample. Theoretical calculations show that up to 1000-fold field enhancement might be achieved for optimum conditions of tip-surface geometry and excitation frequency, leading to increases of the Raman intensities by up to 12 orders of magnitude [15–18]. Experimentally, however, the reported relative change of Raman intensity with and without the tip, $q = I_{\text{TERS}}/I_{\text{RS}}$, has thus far been rather moderate, varying only between 1.4 and 40 [7–14]. If the reduced surface area probed by TERS is taken into account, this corresponds to local enhancements of the Raman intensity of less than about 10^4 . In this Letter, we report on giant tip-enhanced Raman effects, where an up to 10^6 -fold increase of the Raman intensity is observed, arising from a surface area smaller than 100 nm in radius. It is believed that

in this way the avenue is opened for a microscopic technique for vibrational spectroscopy of adsorbed species on the nanometer length scale.

The principle of the experimental arrangement is depicted in Fig. 1. Light from a He-Ne laser ($\lambda_{\text{ex}} = 632.8$ nm) passes through a $50\times$ long distance objective of an Olympus microscope and is directed onto the sample surface at an angle of 60° . The backscattered light is collected through the same objective and transferred through a notch filter into the Raman spectrograph (LabRam 1000). The positions of the surface and the STM head can be adjusted with respect to the laser focus by x - and y -translation stages. The movement of the STM tip towards the surface is performed first by a mechanical coarse approach and then by electronic feedback, controlling a piezotube. Focusing of the light as well as the coarse approach of the tip to the sample are monitored and controlled with an auxiliary camera. The

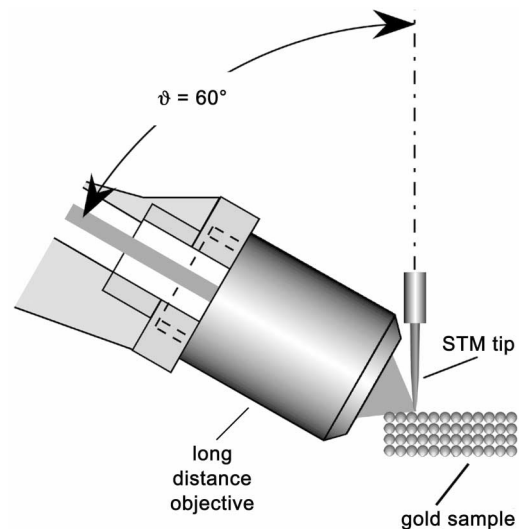


FIG. 1. Experimental setup for TERS using the 60° arrangement. Olympus long distance microscope: $50\times$ magnification, $\text{NA} = 0.5$. He-Ne laser: 5 mW at the sample, $\lambda_{\text{ex}} = 632.8$ nm.

experiments were performed with smooth Au(111) and Pt(110) surfaces, which had been prepared by the flame-annealing technique [19]. The STM tip was in most cases prepared from a gold wire of 0.25 mm diameter by electrochemical etching in a (1:1) mixture of ethanol and concentrated HCl, yielding typical tip radii of about 40–60 nm [12,20]. STM images recorded with either Au or Ir tips showed that the surfaces studied were rather smooth, exhibiting essentially only monatomic steps. Since our present configuration, a tip-adsorbate-metal configuration, is operated in air and not under UHV conditions, detailed information about the chemical state of the sample surfaces is not available.

If the STM tip is brought into the tunneling position at about 1 nm distance above the surface (without accidental contact), an optical cavity is formed. Localized surface plasmons (LSP) can be excited by proper illumination, i.e., if this cavity is placed into the focus of the laser light. The LSP are associated with electron density oscillations under the influence of the external electromagnetic field, creating in turn their own electromagnetic field. Molecules exposed to this enhanced field in close vicinity to the tip apex contribute to the TERS effect, which is therefore locally restricted.

The first example to be presented concerns CN^- ions adsorbed on a Au(111) surface. These ions were adsorbed in an electrochemical environment under potential control (-0.75 V vs saturated calomel electrode) forming a monolayer, which remained stable even after emersion of the sample from a $0.1M$ $\text{NaClO}_4 + 0.001M$ NaCN solution. With visible light, cyanide ions in solution or in the solid state exhibit only normal Raman scattering with a very minute cross section of about $4 \times 10^{-30} \text{ cm}^2 \text{ sr}^{-1}$ in aqueous solution. In Fig. 2, the bottom curve shows a Raman spectrum of a monolayer of CN^- on Au(111) with the tip retracted. No signal can be detected in the CN-stretch spectral region because the Raman sensitivity is far too low under these conditions. Indeed, assuming a cross section of $4 \times 10^{-30} \text{ cm}^2 \text{ sr}^{-1}$ also for the surface species [thus not considering a possible charge transfer enhancement mechanism for CN^- at Au(111)], an incident laser power of 5 mW, a surface density of $8 \times 10^{14} \text{ CN}^- \text{ ions cm}^{-2}$, and an overall efficiency of the spectrometer system of $\eta = 0.005$, the normal Raman intensity is estimated to be 0.25 cps, which is below our detection limit. When the tip is moved into the tunneling distance, the situation changes remarkably. As shown in Fig. 2, upper trace, a pronounced peak centered at 2144 cm^{-1} appears, which is characteristic for the CN^- stretch vibration.

Under the applied conditions, the intensity of the CN-stretch vibration has an integral intensity of about 200 cps. If we assume a localization of the field to the geometric tip size with a radius of 40 nm (from scanning electron microscopy (SEM) images, not shown) [7,11], this intensity corresponds to a TERS enhancement of

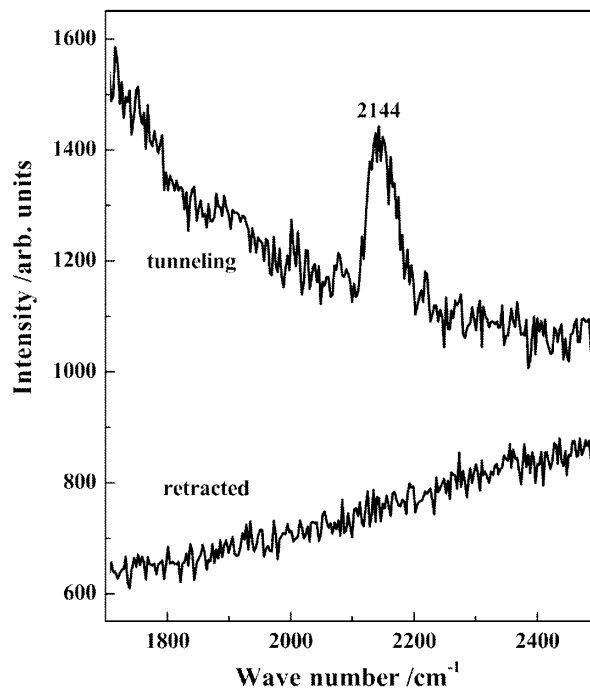


FIG. 2. TERS for CN^- at Au(111). Bottom curve for the tip-retracted case and top curve for the tip-tunneling case. Cyanide ions adsorbed from an aqueous $10^{-3}M$ $\text{NaCN} + 0.1M$ NaClO_4 solution. Acquisition time: 30 s. Laser power: 5 mW. Adsorption and emersion potential: -0.75 V vs SCE. Tunneling current: 1 nA; voltage: -150 mV.

about 4×10^5 in comparison with the Raman intensity of CN^- in aqueous solution.

Since with CN^- on Au(111) no signal was discernible at all with the tip retracted, the actual enhancement cannot be experimentally determined. For a quantitative determination of the Raman enhancement, a dye molecule, malachite green isothiocyanate (MGITC), was used as adsorbate. MGITC exhibits intrinsic signal enhancement by resonance Raman scattering (RRS), if a suitable excitation energy is used, such as the 632.8 nm He-Ne laser line. Furthermore, fluorescence of the adsorbed dye is effectively quenched by the metal surface. Figure 3 shows data for MGITC adsorbed on a Au(111) surface in the presence of an Ir tip, as well as adsorbed on a Pt(110) surface in combination with a Au tip. In the former case with the tip retracted, a weak Raman spectrum is observed due to RRS with integral intensities of about 2–5 cps for the strongest bands (trace *c*). This intensity decays slowly with time due to light-induced bleaching of the adsorbed dye. When the Ir tip is brought into the tunneling position, the Raman intensity increases by a factor of 2 (trace *d*). Considering that the field enhancement is restricted to the apex of the Ir tip, which covers only a small fraction of the laser focus, we estimate a moderate local Raman intensity enhancement. We conclude that the Ir tip/Au(111) cavity supports the excitation of LSP, although with significant damping.

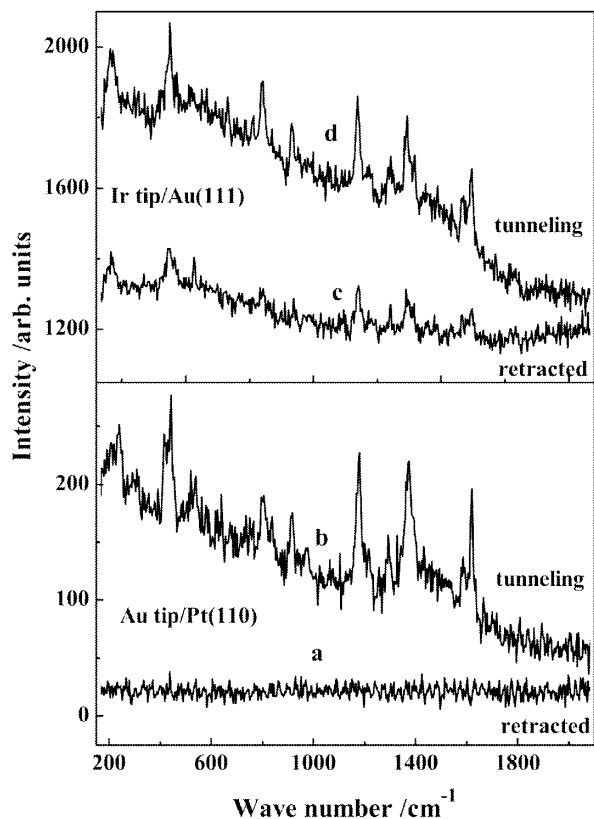


FIG. 3. TERS and RRS for other tip-metal configurations. Top panel: Ir tip/Au(111); acquisition time 30 s. Bottom panel: Au tip/Pt(110); acquisition time 2 s. For both configurations, the MGITC dye is adsorbed from a $10^{-6}M$ ethanol solution for 30 min. Laser power: 5 mW. Tunneling current: 1 nA; voltage: -150 mV.

MGITC on a Pt(110) surface with the tip retracted shows no RRS signal (Fig. 3, trace *a*). Presumably, this is due to, compared to gold, a lower surface intensity and reflectivity. However, in the presence of a Au tip a pronounced spectrum (trace *b*) is produced, signalling the amplification of the overall Raman intensity by several orders of magnitude, similar to the results above with CN^- on Au(111). Obviously, the choice of the tip material is essential for the generation of localized surface plasmons.

The quantification of the enhancement in the presence of the tip becomes possible for MGITC on Au(111). In the absence of the tip only RRS is active, producing a weak signal as shown in Fig. 4, lower trace. The integral intensities reach about 1–2 cps for the strongest bands. The intensity of the 1618 cm^{-1} band decays with a time constant of about $\tau_{\text{RRS}} = 800$ s because of the bleaching of the dye (this value is an average over a number of time series measurements). This situation changes dramatically, if the Au tip is brought into the tunneling position. The strongest Raman peak intensities rose from 1–2 cps to about 5600 to 16 500 cps. For the six strongest bands, the average net increase of the intensity q is about

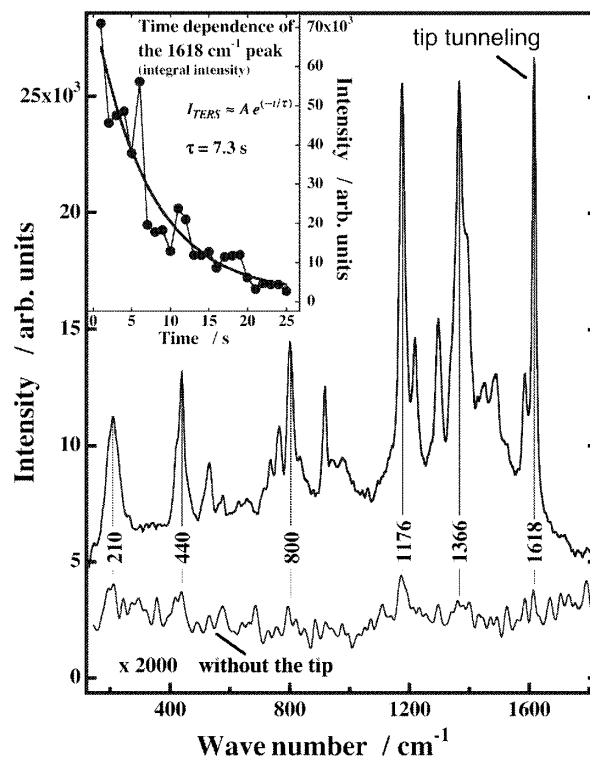


FIG. 4. Comparison of RRS and TERS spectra for malachite green isothiocyanate adsorbed at a Au(111) surface. The laser power in the TERS case is reduced to 0.5 mW; the spectral intensities are normalized to full laser power (5 mW) and acquisition time 1 s. The actual acquisition times were TERS, 1 s and RRS, 60 s. The MGITC dye is adsorbed from a $10^{-7}M$ ethanol solution for 30 min. Tunneling current: 1 nA; voltage: -150 mV. Inset: Time dependence of the integral intensity of the 1618 cm^{-1} band for the reduced laser power.

$q = 8000$, varying for the individual bands between 4000 and 14 000. The different relative enhancement may be attributed to different selection rules occurring in the enhanced field. For recording those data and in order to avoid very rapid bleaching, the laser power had to be reduced to 1/10 of the full power (5 mW), while full laser power was used for recording the lower trace in Fig. 4. For convenience, all intensities in Fig. 4 are normalized to full laser power and 1 s accumulation time.

The enhanced bleaching, due to the intensified field near the tip apex, permits for the first time a direct and rather accurate derivation of the effective field enhancement. The inset of Fig. 4 shows the time dependence of the 1618 cm^{-1} band, assigned to the in-phase stretching of the phenyl rings [21,22]. The intensities are integral intensities, determined over this narrow band. A time constant of $\tau_{\text{TERS}} = 7.3$ s was determined for 1/10 of the full laser power. The time constant for the bleaching of MGITC will be inversely proportional to the local intensity. In the absence of the tip, the time constant τ_{RRS} is $\tau_{\text{RRS}} = 1/I_L \gamma$ where I_L is the laser power in the focus and γ is the bleaching constant. In the presence of the tip, with

an illumination of $I_L/10$ and a local field enhancement factor g (averaged over the probed area, thus implicitly assuming a step function for the field distribution), the time constant is $\tau_{\text{TERS}} = 1/[g^2(I_L/10)\gamma]$. Hence, $10 \times \tau_{\text{RRS}}/\tau_{\text{TERS}} = g^2$ and $g \approx 33$. Since the Raman enhancement F_{TERS} scales approximately with the fourth power of the field enhancement [23], we obtain $F_{\text{TERS}} \approx g^4 \approx 10^6$. The overall enhancement of the Raman signal stems from the field enhancement over a radius a in the vicinity of the tip apex. This area is only a small fraction of the area of the laser focus with the radius R_f . Therefore, from the intensity ratio at $t = 0$ we have $q = I_{\text{TERS}}/I_{\text{RRS}} \approx g^4 a^2 / R_f^2$. With $R_f = 1000$ nm, the radius of the area of the sample probed by TERS results in $a \approx 90$ nm. If the local field distribution were approximated by functions other than a step function, for example by a Gaussian or a Lorentzian profile, the above equation for a would be the same apart from a somewhat altered prefactor. Thus, the estimates would be numerically slightly different, while the general picture would be unaffected.

Note that, for the alignment of tip and sample into the laser focus, the cavity has to be illuminated with the He-Ne laser, although with reduced intensity. During this alignment procedure, we cannot rule out some bleaching of the dye, particularly in the close vicinity of the tip apex. Therefore, the above determined bleaching time constant is rather an upper limit and the effective radius a of the field enhancement might be overestimated. Assuming a slightly reduced time constant of $\tau_{\text{TERS}} \approx 3$ s leads to $g \approx 53$, $F_{\text{TERS}} \approx 7 \times 10^6$, and $a \approx 34$ nm. The actual tip radius of 40 nm, determined by SEM for the tip used in this experiment, comes close to the above estimate. It should be emphasized that the amplification of the Raman signal depends critically on the tip shape. In a number of experiments with different tips, the amplification varied between ~ 100 and 15 000. Although a detailed investigation of the influence of the tip shape is still missing, we observe the tendency that sharper tips yield higher q . Additionally, the tip material is of crucial importance for the undamped excitations of LSP.

As demonstrated in the present paper for CN^- on Au(111), the application of suitable Au tips allowed us to record, for the first time, Raman spectra of an optically nonresonant species on a flat, single crystalline surface, indicating local enhancement factors on the order of 4×10^5 . A direct measurement of the TERS enhancement becomes accessible when using the bleaching behavior of the dye malachite green isothiocyanate (MGITC) adsorbed at Au(111). The presence of the tip considerably increased the bleaching rate due to the local field enhancement. TERS enhancements of up to 10^6 were deter-

mined, extending over an area with less than 100 nm radius. Therefore, in TERS, the optical spectroscopic information stems from a region much smaller than the wavelength of the light used.

B. R. gratefully acknowledges support from the Alexander von Humboldt Foundation, and G. P. a scholarship by the Max-Planck-Society.

*Electronic address: pettinger@fhi-berlin.mpg.de

- [1] W. Ho, *J. Chem. Phys.* **117**, 11033 (2002).
- [2] H. J. Lee and W. Ho, *Science* **286**, 1719 (1999).
- [3] A. J. Meixner, D. Zeisel, M. A. Bopp, and G. Tarrach, *Opt. Eng.* **34**, 2324 (1995).
- [4] J. Azoulay, A. Debarre, A. Richard, and P. Tchenio, *J. Microsc.* **194**, 486 (1999).
- [5] F. Vargas, O. Hollricher, O. Marti, G. De Schaetzen, and G. Tarrach, *J. Chem. Phys.* **117**, 866 (2002).
- [6] L. Aeschimann, T. Akiyama, U. Staufer, N. F. De Rooij, L. Thiery, R. Eckert, and H. Heinzelmann, *J. Microsc.* **209**, 182 (2003).
- [7] R. M. Stöckle, Y. Doug Suh, V. Deckert, and R. Zenobi, *Chem. Phys. Lett.* **318**, 131 (2000).
- [8] M. S. Anderson, *Appl. Phys. Lett.* **76**, 3130 (2000).
- [9] N. Hayazawa, Y. Inouye, Z. Sekhat, and S. Kawata, *J. Chem. Phys.* **117**, 1296 (2002).
- [10] L. T. Nieman, G. M. Krampert, and R. E. Martinez, *Rev. Sci. Instrum.* **72**, 1691 (2001).
- [11] B. Pettinger, G. Picardi, R. Schuster, and G. Ertl, *Single Molecules* **3**, 285 (2002).
- [12] B. Pettinger, G. Picardi, R. Schuster, and G. Ertl, *J. Electroanal. Chem.* **554**, 293 (2003).
- [13] N. Hayazawa, T. Yano, H. Watanabe, Y. Inouye, and S. Kawata, *Chem. Phys. Lett.* **376**, 174 (2003).
- [14] A. Hartschuh, E. J. Sanchez, X. S. Xie, and L. Novotny, *Phys. Rev. Lett.* **90**, 095503 (2003).
- [15] J. Jersch, F. Demming, L. J. Hildenhagen, and K. Dickmann, *Appl. Phys. A* **66**, 29 (1998).
- [16] F. Demming, J. Jersch, K. Dickmann, and P. I. Geshev, *Appl. Phys. B* **66**, 593 (1998).
- [17] M. Micic, N. Klymyshyn, Y. D. Suh, and H. P. Lu, *J. Phys. Chem. B* **107**, 1574 (2003).
- [18] D. Hu, M. Micic, N. Klymyshyn, Y. D. Suh, and H. P. Lu, *Rev. Sci. Instrum.* **74**, 3347 (2003).
- [19] J. Clavilier, R. Faure, G. Guinet, and R. Durand, *J. Electroanal. Chem.* **107**, 205 (1980).
- [20] B. Ren, G. Picardi, and B. Pettinger (to be published).
- [21] S. Schneider, G. Brehm, and P. Freunshcht, *Phys. Status Solidi B* **189**, 37 (1995).
- [22] W. E. Doering and S. M. Nie, *Anal. Chem.* **75**, 6171 (2003).
- [23] M. Kerker, D. S. Wang, and H. Chew, *Appl. Opt.* **19**, 3373 (1980).